First-Principles Study of Electric Field Effects on Magnetic Anisotropy in ultrathin ferromagnetic TM (TM=Fe, Co) films on Pt(111) underlayer

Shugo Suzuki, Masashi Shiota, Yasushi Fukuchi, and Saori Seki

Division of Materials Science, Faculty of Pure and Applied Sciences, University of Tsukuba, Tsukuba, Ibaraki 305-8573, Japan

We study the electric field (EF) effects on the magnetic anisotropy in the ultrathin ferromagnetic TM (TM=Fe, Co) films on the Pt(111) underlayer using relativistic first-principles calculations based on the density functional theory with a special attention on the effects of Pt segregation. The magnetic anisotropy energy, MAE, and the spin magnetic moment, $M_{\rm spin}$, of the Pt/TM/Pt(111) and BeO/Pt/TM/Pt(111) systems as well as those of the TM/Pt(111) and BeO/TM/Pt(111) systems are calculated in the absence of or under the EF. It is found that the MAE and its EF dependence of the BeO/Pt/TM/Pt(111) systems, especially those of the BeO/Pt/Co/Pt(111) system, are considerably large. The sign of the EF dependence is such that the MAE and $M_{\rm spin}$ are increased (decreased) when the EF increases (decreases) the number of electrons in the system. We attribute this unique behavior to the formation of the hybridized majority-spin states originated in the O $2p_z$, Pt $5d_{3z^2-r^2}$, and TM $3d$ orbitals of the interfacial atoms.

1. Introduction

Recently ultrathin ferromagnetic films have attracted much attention not only because of scientific interest but also because of its potential applications.[1)] Following the work on ferromagnetic semiconductors,[2–4)] the experimental studies of the electric field (EF) control of the magnetic properties of ultrathin ferromagnetic transition metal (TM) films have been done extensively motivated by requirements to achieve ultra-low power consumption of magnetic memory storage devices.[5–28)] The mechanism of the EF effects on the magnetic anisotropy energy, MAE, and the spin magnetic moment, $M_{\rm spin}$, in ultrathin ferromagnetic TM films has also been studied theoretically.[29–41)]

One of the systems of fundamental importance in understanding the EF effects on the magnetic anisotropy is ultrathin ferromagnetic TM films on the Au(001) underlayer capped

with the MgO insulating layer, i.e., the MgO/TM/Au(001) systems. Maruyama et al. found a large voltage-induced magnetic anisotropy change in the MgO/Fe/Au(001) system.[6] They showed that a relatively small EF can cause a large change in the MAE of about 8.4 μJm^{-2} when the applied voltage is changed from 200 V to −200 V. Shiota et al. evaluated the change in the MAE of the MgO/$Fe_{80}Co_{20}$/Au(001) system quantitatively.[8,16] They found that the MAE depends linearly on the EF with a slope of about 30 fJV^{-1}m^{-1}, i.e., 0.015 meV/TM per V/nm. It should be noted that the sign of the EF dependence of the MAE found by Maruyama et al. and Shiota et al. is such that the perpendicular magnetic anisotropy is enhanced by the EF that decreases the number of electrons in the system. Also the EF effects on the MAE of ultrathin ferromagnetic Fe films have been studied theoretically.[29–39] Recently we have shown that the EF dependence of the MAE of the MgO/Fe/Au(001) system is 0.006 meV/Fe per V/nm, which is in a semi-quantitative agreement with the experimental result, 0.015 meV/TM per V/nm, with successful reproduction of the sign of the measured EF dependence.[41]

Another system of fundamental importance is ultrathin ferromagnetic TM films on the Pt(111) underlayer capped with the MgO insulating layer, i.e., the MgO/TM/Pt(111) systems. Chiba et al. showed that the Curie temperature of the MgO/Co/Pt(111) system is increased (decreased) by the EF that increases (decreases) the number of electrons in the system.[13] Furthermore, using the ionic liquid film, the change in the Curie temperature of about 100 K has been achieved with the gate voltage change of ±2 V;[20] the change in the number of electrons per Co atom at the interface induced by this gate voltage was estimated to be about 0.084, which corresponds to the EF of about 23 V/nm. They subsequently studied the EF effects on the MAE, the coercivity, and the magnetization of the MgO/TM/Pt(111) systems.[22,26] In particular, the magnetization measurement clearly showed that the magnetization is increased (decreased) by the EF that increases (decreases) the number of electrons in the system;[20,22] since, in general, a larger magnetization results in a higher Curie temperature,[42] this is consistent with the observed EF dependence of the Curie temperature of the MgO/Co/Pt(111) system.[13,20] It is interesting to note that the sign of the EF dependence of the Curie temperature and the magnetization of the MgO/TM/Pt(111) systems is opposite to the sign of the EF dependence of the MAE of the MgO/TM/Au(001) and MgO/$Fe_{80}Co_{20}$/Au(001) systems although it is not clear what relationship exists among these quantities.

For the surface or interface region of the systems with TM and Pt atoms, one point to be noticed is that Pt can segregate to the surface or interface to form a thin Pt overlayer on top of the TM layer.[43,44] Thus it is important to consider the possibility of Pt segregation in the systems with the ultrathin TM films on the Pt(111) underlayer. There have been pioneer-

ing theoretical studies of the effects of the segregation of the underlayer atoms on the MAE and its EF dependence.[32,38,39] Tsujikawa and Oda calculated the MAE and its EF dependence of the Fe/Pt(001) and Pt/Fe/Pt(001) systems as well as those of the MgO/Fe/Au(001) system.[32,39] Although these studies revealed some important aspects of the effects of segregation in these systems, further theoretical studies are indispensable in understanding the EF effects in the systems with or without Pt segregation, especially the ultrathin Co film on the Pt(111) underlayer.

The purpose of this work is to study the EF effects on the magnetic anisotropy in the ultrathin ferromagnetic TM (TM=Fe, Co) films on the Pt(111) underlayer with or without Pt segregation using relativistic first-principles calculations based on the density functional theory. We study the MAE and $M_{\rm spin}$ and their EF dependence of the Pt/TM/Pt(111) and BeO/Pt/TM/Pt(111) systems as well as those of the TM/Pt(111) and BeO/TM/Pt(111) systems. We describe the method of calculations in Sect. 2. The results and discussion are given in Sect. 3. Finally, we give the conclusions of this work in Sect. 4.

2. Method of Calculations

We examine the MAE and $M_{\rm spin}$ and their EF dependence of the TM/Pt(111), Pt/TM/Pt(111), BeO/TM/Pt(111), and BeO/Pt/TM/Pt(111) systems. For all the systems studied in this work, we consider a single TM monolayer as the ferromagnetic layer in each system adopting a unit cell with a single TM atom. The underlayer consists of two Pt monolayers and the insulating layer consists of two Be and two O monolayers. The reason why we adopted BeO instead of MgO as the insulating layer is the small lattice mismatch, less than 3%, between the lattice constants of the (111) plane of fcc Pt and the basal plane of wurtzite BeO. The schematic diagram of the BeO/Pt/TM/Pt(111) is shown in Fig. 1.

We employ all-electron calculations using the scalar relativistic full-potential linear-combination-of-atomic-orbitals (SFLCAO) method and the fully relativistic full-potential linear-combination-of-atomic-orbitals (FFLCAO) method, both based on the density functional theory.[45–47] We adopted the local spin density approximation using the Perdew-Wang parameterization of the Ceperley-Alder results as the exchange-correlation energy functional.[48,49] Also, to calculate the electrostatic potential, we used the two-dimensional Ewald method.[50,51] We first optimized the structure of the system using the SFLCAO method in the absence of or under the EF; in the SFLCAO method, both core and valence states are calculated using an appropriate averaging procedure of the spin-orbit coupling.[47] With the optimized structure, we next calculated the MAE of the system using the FFLCAO method in

the absence of or under the EF; in the FFLCAO method, we solve the Kohn-Sham equations of the Dirac type not only for core states but also for valence states, thereby taking account of all the relativistic effects including the spin-orbit coupling.[46)]

The EF was applied as follows. We consider a counter electrode placed far above the system and charged oppositely to the charge state of the system. That is, we introduce the following external potential originated in the counter electrode:

$$V_{\mathrm{CE}}(z) = -\frac{2\pi e^2 \Delta N}{A_{\mathrm{cell}}} z \ . \tag{1}$$

Here A_{cell} is the area of the unit cell: $A_{\mathrm{cell}} = \sqrt{3}a^2/2$ with $a = 2.77$ Å being the in-plane lattice constant of the triangular lattice of the Pt(111) underlayer. Also ΔN represents the change in the number of electrons in the unit cell of the system and the EF is given by $-0.272\,\Delta N \times 10^3$ V/nm. In this work, we consider ΔN=−0.1, 0.0, and 0.1, which correspond to the EF of 27.2, 0.0, and −27.2 V/nm, respectively. The magnitude of the EF considered in this work is close to that of the EF applied in the experiment employing the ionic liquid film, about 23 V/nm. Note that one half of the EF is originated in the counter electrode while the other half is originated in the system itself. We define the direction of the EF in such a way that a positive (negative) EF decreases (increases) the number of electrons in the system; in other words, a positive (negative) EF corresponds to a negative (positive) voltage applied to the counter electrode with respect to the system. We calculated the MAE as well as M_{spin} in the absence of or under the EF using the FFLCAO method. The MAE calculated in this work is the difference between the total energy for the in-plane magnetization, $E_{\mathrm{tot}}^{[1\bar{1}0]}$, and that for the perpendicular magnetization, $E_{\mathrm{tot}}^{[111]}$. We adopt the definition that the positive (negative) MAE corresponds to the perpendicular (in-plane) magnetic anisotropy, i.e., MAE=$E_{\mathrm{tot}}^{[1\bar{1}0]} - E_{\mathrm{tot}}^{[111]}$. We do not consider the contribution of the shape magnetic anisotropy originated in the magnetic dipole-dipole interaction.

We determined the structures of the systems as follows. The x and y coordinates of the atoms in the system were chosen according to the in-plane lattice constant of the triangular lattice of the Pt(111) underlayer; the in-plane primitive vectors are $\boldsymbol{a}_1 = (a, 0, 0)$ and $\boldsymbol{a}_2 = (-a/2,\ \sqrt{3}a/2, 0)$. In this work, we assume that the TM atom is at the hcp hollow site of the Pt(111) underlayer. Also, for the BeO/TM/Pt(111) and BeO/Pt/TM/Pt(111) systems, we consider the geometry where the interfacial O atom is on top of the interfacial metal atom, the TM or Pt atom, rather than at the hollow site surrounded by the metal atoms. For the Pt/TM/Pt(111) and BeO/Pt/TM/Pt(111) systems, we also assume that the segregated Pt atom is at the hcp hollow site; that is, we assume that the segregated Pt atom has the same x and

y coordinates as those of the Pt atom directly under the TM layer. The z coordinates of the constituent atoms were optimized using the SFLCAO method. We fixed the center of mass of the system during the optimization and used the force criterion for stopping the structure optimization of 0.01 eV/Å.

The atomic orbitals used as the basis functions are as follows: the 1s and 2s orbitals of the neutral Be atom, the 2p orbitals of the Be^{+} atom, the 2s orbitals of the Be^{2+} atom, the 2p and 3d orbitals of the Be^{3+} atom, the 1s, 2s, and 2p orbitals of the neutral O atom, the 2s and 2p orbitals of the O^{2+} atom, the 3d orbitals of the O^{6+} atom, the 1s, 2s, 2p, 3s, 3p, 3d, and 4s orbitals of the neutral TM atom, the 3d, 4s, and 4p orbitals of the TM^{2+} atom, the 1s, 2s, 2p, 3s, 3p, 3d, 4s, 4p, 4d, 4f, 5s, 5p, 5d, and 6s orbitals of the neutral Pt atom, and the 5d, 6s, and 6p orbitals of the Pt^{2+} atom. It is worth noting that the use of the atomic orbitals of positively charged atoms as well as those of neutral atoms is crucial to the description of the contraction of atomic orbitals associated with cohesion. Also, to terminate the dangling bond of the Be atom in the top insulating layer, we adopted the fictitious atom method;[52,53] the fictitious atom used in our calculations consists of a nuclear charge of $+1.5e$ and an electronic charge of $-1.5e$ with the atomic orbitals of the hydrogen atom. The Brillouin-zone integration was carried out using the good-lattice-point method;[54] we used 34 $\boldsymbol{k}$ points for the structure optimization and 987 $\boldsymbol{k}$ points for the calculations of the MAE. To speed up the convergence, we used a Fermi distribution smearing of eigenstates with a width of 30 meV.

For the BeO/TM/Pt(111) and BeO/Pt/TM/Pt(111) systems, we should examine the perpendicular component of the electric dipole moment of the unit cell, p_z, and the associated internal EF in the BeO insulating layer, $E_{\rm int}$, because this can exist due to the lack of the inversion symmetry in wurtzite BeO. We calculated p_z and estimated $E_{\rm int}$ using p_z as follows. The calculated p_z is about 0.5×10^{-30} Cm = 0.2 D. Assuming the thickness of the BeO insulating layer, d, to be 4 Å and using $E_{\rm int} = 4\pi p_z / A_{\rm cell} d$, $E_{\rm int}$ is estimated to be about 2 V/nm. This is sufficiently small in comparison with the external EF considered in this work, 27.2 V/nm, and may not affect the results of calculations.

3. Results and Discussion

3.1 TM/Pt(111) systems

In Table I, we show the calculated MAE and $M_{\rm spin}$ of the TM/Pt(111), Pt/TM/Pt(111), BeO/TM/Pt(111), and BeO/Pt/TM/Pt(111) systems. For comparison, we also show those of the freestanding Fe(111) and Co(111) monolayer systems with the lattice constant taken to match the Pt(111) underlayer.[41]

We begin with the Fe/Pt(111) system in the absence of the EF. The MAE of the Fe/Pt(111) system, −0.24 meV/cell, is negative, showing an in-plane magnetic anisotropy. This is in contrast to the perpendicular magnetic anisotropy of the freestanding Fe(111) monolayer system, 0.21 meV/cell. Also $M_{\rm spin}$ of the Fe/Pt(111) system, 3.39 $\mu_{\rm B}$, is larger by about 0.3 $\mu_{\rm B}$ than that of the freestanding Fe(111) monolayer system, 3.10 $\mu_{\rm B}$. The enhancement of $M_{\rm spin}$ is due to the high magnetic polarizability of Pt. We found by the Mulliken population analysis that the contribution of the Fe atom to $M_{\rm spin}$ is 3.00 $\mu_{\rm B}$ while that of the Pt atom adjacent to the Fe atom is 0.33 $\mu_{\rm B}$.

The in-plane magnetic anisotropy and the enhancement of $M_{\rm spin}$ in the Fe/Pt(111) system in the absence of the EF were also found by previous theoretical studies. The MAE and $M_{\rm spin}$ calculated by Tsujikawa et al. are −0.4 meV/Fe atom and 3.1 $\mu_{\rm B}$, respectively.[55] Moulas et al. obtained the MAE of about −0.7 meV/Fe atom and $M_{\rm spin}$ of 3.2 $\mu_{\rm B}$.[56] Lehnert et al. found that the MAE and $M_{\rm spin}$ are −0.6 meV/Fe atom and 3.4 $\mu_{\rm B}$, respectively.[57] On the other hand, in contrast to the theoretical results, the experimentally measured MAE of the Fe/Pt(111) system indicates a perpendicular magnetic anisotropy with a positive value of about 0.1 meV/Fe atom.[56] A possible origin of the discrepancy between the theoretical and experimental results is that a thin Fe film can show complex magnetic structures with prevalent antiferromagnetic order.[56] Another possible origin is that the Fe atom is incorporated into the Pt top layer as pointed out by Repetto et al.[58]

When the positive (negative) EF is applied, the MAE of the Fe/Pt(111) system is increased (decreased) to be 0.47 (−0.59) meV/cell and $M_{\rm spin}$ is also increased (decreased) to be 3.45 (3.28) $\mu_{\rm B}$. For the positive EF, the system shows a perpendicular magnetic anisotropy. The EF dependence of the MAE is about 0.02 meV/cell per V/nm. This is close to the EF dependence of the MAE of the Fe/Pt(001) system obtained by Tsujikawa and Oda, 0.03 meV/cell per V/nm, although the surface orientation is different.[32] We found by the Mulliken population analysis that the change in $M_{\rm spin}$ is due to the change in the number of the minority-spin electrons, which is mostly originated in the Fe 3*d* electrons.

We next consider the Co/Pt(111) system. In the absence of the EF, our calculated MAE, 0.24 meV/cell, is positive, showing a perpendicular magnetic anisotropy. This is in contrast to the in-plane magnetic anisotropy of the freestanding Co(111) monolayer system, −1.43 meV/cell. It is also found that $M_{\rm spin}$ of the Co/Pt(111) system, 2.54 $\mu_{\rm B}$, is larger by about 0.5 $\mu_{\rm B}$ than that of the freestanding Co(111) monolayer system, 2.06 $\mu_{\rm B}$. The enhancement of $M_{\rm spin}$ is again due to the high magnetic polarizability of Pt. We found by the Mulliken population analysis that the contribution of the Co atom to $M_{\rm spin}$ is 2.01 $\mu_{\rm B}$ while that of the

Pt atom adjacent to the Co atom is 0.39 μ_B.

The perpendicular magnetic anisotropy and the enhancement of M_{spin} in the Co/Pt(111) system in the absence of the EF were also found by previous theoretical studies. The MAE and M_{spin} calculated by Moulas et al. are 0.1 meV/Co atom and 2.2 μ_B, respectively.[56] Lehnert et al. obtained the MAE of 0.6 meV/Co atom and M_{spin} of 2.5 μ_B, where the contributions of the Co atom and the adjacent Pt atom are 2.0 and 0.4 μ_B, respectively.[57] The experimentally measured MAE of the Co/Pt(111) system is about 0.15 meV/Co atom, showing a perpendicular magnetic anisotropy.[56] The agreement between the theoretical and experimental results is reasonable.

When the positive (negative) EF is applied, the MAE of the Co/Pt(111) system is decreased (increased) to be −0.41 (0.68) meV/cell and M_{spin} is increased (decreased) to be 2.61 (2.49) μ_B. For the positive EF, the system shows an in-plane magnetic anisotropy. The EF dependence of the MAE is about −0.02 meV/cell per V/nm, which is close to that of the Fe/Pt(111) system in magnitude but with the opposite sign. We found by the Mulliken population analysis that the change in M_{spin} is again due to the change in the number of the minority-spin electrons, which is mostly originated in the Co 3*d* electrons.

3.2 Pt/TM/Pt(111) systems

In comparison to the Fe/Pt(111) system, the calculated MAE of the Pt/Fe/Pt(111) system is considerably increased by the existence of the segregated Pt atom; the MAE of the Pt/Fe/Pt(111) system is 3.69 meV/cell in the absence of the EF while 4.52 (2.71) meV/cell for the positive (negative) EF. The EF dependence of the MAE is about 0.03 meV/cell per V/nm. We also find that, in contrast to the Fe/Pt(111) system, M_{spin} of the Pt/Fe/Pt(111) system is almost unaffected by the EF.

The enhancement of the MAE by the segregated Pt atom is in agreement with the enhancement of the MAE of the Pt/Fe/Pt(001) system to that of the Fe/Pt(001) system found by Tsujikawa and Oda; the MAE of the Fe/Pt(001) system is small in magnitude, less than 0.1 meV/Fe atom, while that of the Pt/Fe/Pt(001) system is large, about 5 meV/Fe atom.[32] The EF dependence of the MAE of the Pt/Fe/Pt(111) system found in this work, about 0.03 meV/cell per V/nm, is almost the same as the one found for the Fe/Pt(111) system, 0.02 meV/cell. Also our result is close to the the EF dependence of the MAE of the Pt/Fe/Pt(001) system calculated by Tsujikawa and Oda, 0.035 meV/Fe atom per V/nm.[32]

For the Pt/Co/Pt(111) system, the calculated MAE is also increased by the existence of the segregated Pt atom; the MAE of the Pt/Co/Pt(111) system is 0.95 meV/cell in the absence

of the EF while 2.37 (1.15) meV/cell for the positive (negative) EF. The EF dependence of the MAE of the Pt/Co/Pt(111) system is not linear; it is about 0.05 meV/cell per V/nm for the positive EF while about −0.01 meV/cell per V/nm for the negative EF. We also find that $M_{\rm spin}$ of the Pt/Co/Pt(111) system is increased (decreased) by the positive (negative) EF by 0.06 (0.05) $\mu_{\rm B}$. The calculated MAE are slightly smaller than those of the Pt/Fe/Pt(111) systems.

3.3 BeO/TM/Pt(111) systems

We next consider the BeO/Fe/Pt(111) system. In comparison to the Fe/Pt(111) system, the calculated MAE is increased by the existence of the BeO insulating layer; the MAE of the BeO/Fe/Pt(111) system is 0.60 meV/cell in the absence of the EF while 0.73 (0.59) meV/cell for the positive (negative) EF. The EF dependence of the MAE is small; it is about 0.005 meV/cell per V/nm for the positive EF while almost no EF dependence for the negative EF. The calculated $M_{\rm spin}$ of the BeO/Fe/Pt(111) system is almost the same as those of the Fe/Pt(111) system; $M_{\rm spin}$ of the BeO/Fe/Pt(111) system is 3.40 $\mu_{\rm B}$ in the absence of the EF while 3.47 (3.32) $\mu_{\rm B}$ for the positive (negative) EF. We found by the Mulliken population analysis that the change in $M_{\rm spin}$ is due to the change in the number of the minority-spin electrons, which is mostly originated in the Fe 3*d* electrons. The suppression of the EF dependence of the MAE is likely due to the formation of a strong covalent bond between the O and Fe atoms as found in the MgO/Fe/Au(111) system.[41)]

For the BeO/Co/Pt(111) system, the calculated MAE is considerably increased by the existence of the BeO insulating layer; the MAE of the BeO/Co/Pt(111) system is 3.56 meV/cell in the absence of the EF while 3.80 (3.60) for the positive (negative) EF. However, the EF dependence of the MAE is also small; it is less than 0.01 meV/cell per V/nm for the positive EF while almost no EF dependence for the negative EF. $M_{\rm spin}$ of the BeO/Co/Pt(111) system is almost the same as those of the Co/Pt(111) system; it is found that $M_{\rm spin}$ of the BeO/Co/Pt(111) system is 2.58 $\mu_{\rm B}$ in the absence of the EF while 2.62 (2.56) $\mu_{\rm B}$ for the positive (negative) EF. We found by the Mulliken population analysis that the change in $M_{\rm spin}$ is again due to the change in the number of the minority-spin electrons, which is mostly originated in the Co 3*d* electrons. The suppression of the EF dependence of the MAE is again likely due to the formation of a strong covalent bond between the O and Co atoms as found in the MgO/Co/Au(111) system.[41)]

3.4 BeO/Pt/TM/Pt(111) systems

We find that the MAE and its EF dependence of the BeO/Pt/Fe/Pt(111) system is considerably large; the calculated MAE is 3.63 meV/cell in the absence of the EF while 1.27 (4.67) meV/cell for the positive (negative) EF; the EF dependence of the MAE is −0.06 meV/cell per V/nm. The calculated $M_{\rm spin}$ is 3.22 $\mu_{\rm B}$ in the absence of the EF and 3.14 (3.34) $\mu_{\rm B}$ for the positive (negative) EF. It is important to note that the sign of the EF dependence of the MAE and $M_{\rm spin}$ is such that they are decreased (increased) by the positive (negative) EF.

For the BeO/Pt/Co/Pt(111) system, we find that the MAE and its EF dependence of the BeO/Pt/Co/Pt(111) system is extremely large; the calculated MAE is 13.64 meV/cell in the absence of the EF while 10.34 (15.10) meV/cell for the positive (negative) EF. This is comparable to the giant MAE of 9 meV/Co atom observed in the system of single Co atoms deposited on the Pt(111) underlayer.[59] The EF dependence of the MAE is −0.09 meV/cell per V/nm. The calculated $M_{\rm spin}$ is 2.99 $\mu_{\rm B}$ in the absence of the EF and 2.81 (3.08) $\mu_{\rm B}$ for the positive (negative) EF. It is important to note again that the sign of the EF dependence of the MAE and $M_{\rm spin}$ is such that they are decreased (increased) by the positive (negative) EF; this is the same EF dependence found for the BeO/Pt/Fe/Pt(111) system.

The important point to be noticed is that the sign of the EF dependence of $M_{\rm spin}$ is opposite to that found in the other systems studied in this work and our previous work.[41] This unique behavior of $M_{\rm spin}$ may be related to the origin of the EF dependence of the MAE of the BeO/Pt/TM/Pt(111) systems. To check whether the EF dependence of the MAE and $M_{\rm spin}$ is affected by the structure relaxation caused by the EF, we calculated the MAE and $M_{\rm spin}$ using the same structure as the one obtained in the absence of the EF. The results given in Table I clearly show that the origin of the unique behavior is almost purely electronic because the MAE and $M_{\rm spin}$ are affected only very slightly by the structure relaxation caused by the EF. It should be noted that this does not mean that the structure relaxation caused by the EF is very small in the BeO/Pt/TM/Pt(111) system. We show the optimized structure of the system in Table II. It is found that the interatomic distance between the segregated Pt atom and the adjacent O atom is changed notably by the EF; it is decreased (increased) by about 0.05 (0.07) Å when the positive (negative) EF is applied. Nevertheless the MAE and $M_{\rm spin}$ are almost unaffected by the structure relaxation caused by the EF.

We carried out the Mulliken population analysis to reveal the details of the EF dependence of $M_{\rm spin}$.[60] The results are shown in Table III. In the table, we show the numbers of majority- and minority-spin electrons, N^+ and N^-, and the difference, $N^+ - N^-$, which represents the

atomic spin magnetic moment in unit of μ_B, of the O atom on top of the segregated Pt atom, the segregated Pt atom, the TM atom, and the first and second Pt atoms in the underlayer. It is found that the change in M_{spin} caused by the EF is mainly due to the following two origins. One is the decrease (increase) in N^+ of the segregated Pt atom and the TM atom while the other is the increase (decrease) in N^- of the TM atom caused by the positive (negative) EF. For TM=Fe, the spin magnetic moment of the segregated Pt atom is 0.20 μ_B in the absence of the EF and 0.16 (0.26) μ_B for the positive (negative) EF. Also the spin magnetic moment of the Fe atom is 2.76 μ_B in the absence of the EF and 2.72 (2.81) μ_B for the positive (negative) EF. For TM=Co, the spin magnetic moment of the segregated Pt atom is 0.41 μ_B in the absence of the EF and 0.33 (0.44) μ_B for the positive (negative) EF. Also the spin magnetic moment of the Co atom is 1.98 μ_B in the absence of the EF and 1.93 (2.01) μ_B for the positive (negative) EF. Note that the spin magnetic moment induced by the TM atom on the segregated Pt atom as well as those induced on the underlayer Pt atoms is much larger for TM=Co than for TM=Fe; this is most likely the reason why the MAE of the BeO/Pt/Co/Pt(111) system is extremely large because the spin-orbit coupling and the resultant magnetic anisotropy in Pt are sizeable. Also it may be worth noting that the spin magnetic moment of the O atom on top of the segregated Pt atom is decreased (increased) by the positive (negative) EF for TM=Fe while almost unchanged irrespective of the EF for TM=Co and that the spin magnetic moments of the underlayer Pt atoms are increased (decreased) by the positive (negative) EF for TM=Fe while decreased (increased) by the positive (negative) EF for TM=Co. This results in a larger EF dependence of M_{spin} for the BeO/Pt/Co/Pt(111) system than for the BeO/Pt/Fe/Pt(111) system.

To understand the origin of the EF dependence of M_{spin} of the BeO/Pt/TM/Pt(111) systems, we examine the partial density of states (PDOS) of the Pt 5d, O 2p, and TM 3d orbitals of the interfacial atoms. The calculated PDOS are shown in Figs. 2-7, where the upper and lower parts of each panel are those for majority- and minority-spin orbitals, respectively. Also each component of the PDOS is labeled with Y_{lm}, a spherical harmonic function of degree l and order m, which is the angular part of the corresponding atomic orbital.

In Figs. 2 and 3, we show the PDOS of the 5d orbitals of the segregated Pt atom in the BeO/Pt/Fe/Pt(111) and BeO/Pt/Co/Pt(111) systems, respectively. In the figures, the PDOS of the Pt 5d orbitals are labeled with Y_{lm} of $l = 2$ and $m = \pm 2, \pm 1$, and 0. Note that Y_{20} represents the Pt $5d_{3z^2-r^2}$ orbital, which lies along the perpendicular direction to the plane of the film. It is found that the PDOS of the majority-spin Pt $5d_{3z^2-r^2}$ orbital contributes dominantly in the vicinity of the Fermi level. The PDOS of the other majority-spin Pt 5d orbitals and all

the minority-spin Pt 5d orbitals are small. The PDOS of the majority-spin Pt 5$d_{3z^2-r^2}$ orbital clearly shows that there exists a peak and the positive (negative) EF pushes up (pulls down) this peak to the high (low) energy side, thereby decreasing (increasing) the number of the majority-spin Pt 5$d_{3z^2-r^2}$ electrons.

In Figs. 4 and 5, we show the PDOS of the 2p orbitals of the interfacial O atom on top of the segregated Pt atom in the BeO/Pt/Fe/Pt(111) and BeO/Pt/Co/Pt(111) systems, respectively. In the figures, the PDOS of the O 2p orbitals are labeled with Y_{lm} of $l = 1$ and $m = \pm 1$ and 0. Note that Y_{10} represents the O 2p_z orbital, which also lies along the perpendicular direction to the plane of the film. It is found that only the PDOS of the majority-spin O 2p_z contributes dominantly in the vicinity of the Fermi level and the shape is very similar to that of the PDOS of the majority-spin Pt 5$d_{3z^2-r^2}$ orbital. This indicates that the majority-spin Pt 5$d_{3z^2-r^2}$ and O 2p_z orbitals hybridize with each other.

In Figs. 6 and 7, we show the PDOS of the 3d orbitals of the TM atoms in the BeO/Pt/Fe/Pt(111) and BeO/Pt/Co/Pt(111) systems, respectively. In the figures, the PDOS of the TM 3d orbitals are labeled with Y_{lm} of $l = 2$ and $m = \pm 2, \pm 1$, and 0. Since the TM atom is not directly under the segregated Pt atom, it may be useful for examining the hybridization with the Pt 5d orbitals to show the total PDOS of the TM 3d orbitals, i.e., the sum of the contributions from the five 3d orbitals for each spin degree of freedom. It is found that the shape of the total PDOS of the majority-spin TM orbitals is also very similar to that of the PDOS of the majority-spin Pt 5$d_{3z^2-r^2}$ orbital. We thus conclude that the majority-spin Pt 5$d_{3z^2-r^2}$, O 2p_z, and TM orbitals hybridize with each other to a considerable degree. In contrast to the PDOS of the Pt 5d and O 2p orbitals shown in Figs. 2-5, there are substantial contributions of the PDOS of the minority-spin TM 3d orbitals. Note that the PDOS of the minority-spin TM 3d orbitals are also changed notably by the EF; this is likely the origin of the increase (decrease) in the number of the minority-spin electrons of the TM atom caused by the positive (negative) EF as found by the Mulliken population analysis although it is difficult to see this quantitatively from the change in the PDOS of the minority-spin TM 3d orbitals caused by the EF shown in Figs. 6 and 7.

Finally, we discuss a possible relation of the results of this work to the experimental observations. Chiba et al. found a large EF dependence of the Curie temperature and the magnetization of the MgO/Co/Pt(111) system.[13,20] The sign of the EF dependence of these quantities is such that they are increased (decreased) by the EF that increases (decreases) the number of electrons in the system in agreement with the sign obtained in this work. This unique EF dependence can be caused by the formation of the hybridized majority-spin states

originated in the interfacial O, Pt, and Co atoms due to the Pt segregation. However, our calculated MAE of the BeO/Pt/Co/Pt(111) system, which is more than 10 meV/cell, is too large in comparison to the experimental MAE, which is estimated to be of the order of 0.1 meV/Co atom at 200 K.[26] One origin of the discrepancy may be that we assume a perfect segregation of the Pt atom on top of the Co layer in the BeO/Pt/Co/Pt(111) system, i.e., a formation of a perfect segregated Pt monolayer. However, the segregation in the real system may not be perfect. Another possible origin is that the interface of the real MgO/Co/Pt(111) system likely contains many types of defect structures that can drastically affect the hybridized majority-spin states originated in the interfacial O, Pt, and Co atoms. In the future, to study the EF effects on the magnetic properties in the real system in more detail, we need to take account of partial Pt segregation and defect structures.

4. Conclusions

We have studied the EF effects on the magnetic anisotropy in the ultrathin ferromagnetic TM films on the Pt(111) underlayer using relativistic first-principles calculations based on the density functional theory with a special attention on the effects of Pt segregation. We have found that the MAE and its EF dependence of the BeO/Pt/TM/Pt(111) systems, especially those of the BeO/Pt/Co/Pt(111) system, are considerably large. The sign of the EF dependence is such that the MAE and $M_{\rm spin}$ is increased (decreased) when the EF increases (decreases) the number of electrons in the system. The origin of the unique EF dependence of $M_{\rm spin}$ of the BeO/Pt/TM/Pt(111) systems is the formation of the hybridized majority-spin states originated in the O $2p_z$, Pt $5d_{3z^2-r^2}$, and TM $3d$ orbitals of the interfacial atoms.

Acknowledgments

We would like to thank D. Chiba for useful comments. We would also like to thank H. Yanagihara for helpful discussions.

Table I. Magnetic anisotropy energy, MAE (in meV/cell), and spin magnetic moment, $M_{\rm spin}$ (in $\mu_{\rm B}$), for the freestanding TM monolayer, TM/Pt(111), Pt/TM/Pt(111), BeO/TM/Pt(111), and BeO/Pt/TM/Pt(111) (TM=Fe, Co) systems for the change in electron number ΔN=−0.1, 0.0, and 0.1. The electric field, EF (in V/nm), is given by $-0.272\,\Delta N \times 10^3$ V/nm, with the definition that a positive (negative) electric field decreases (increases) the number of electrons in the system.

	$\Delta N = -0.1$ (EF = 27.2)		$\Delta N = 0.0$ (EF = 0.0)		$\Delta N = 0.1$ (EF = −27.2)	
System	MAE	$M_{\rm spin}$	MAE	$M_{\rm spin}$	MAE	$M_{\rm spin}$
Fe(111)	0.36	3.18	0.21	3.10	0.32	3.01
Fe/Pt(111)	0.47	3.45	−0.24	3.39	−0.59	3.28
Pt/Fe/Pt(111)	4.52	3.64	3.69	3.64	2.71	3.60
BeO/Fe/Pt(111)	0.73	3.47	0.60	3.40	0.59	3.32
BeO/Pt/Fe/Pt(111)	1.27 1.71[a)]	3.14 3.15[a)]	3.63	3.22	4.67 4.31[a)]	3.34 3.32[a)]
Co(111)	−1.24	2.14	−1.43	2.06	−1.92	1.97
Co/Pt(111)	−0.41	2.61	0.24	2.54	0.68	2.49
Pt/Co/Pt(111)	2.37	2.98	0.95	2.92	1.15	2.87
BeO/Co/Pt(111)	3.80	2.62	3.56	2.58	3.60	2.56
BeO/Pt/Co/Pt(111)	10.34 10.32[a)]	2.81 2.85[a)]	13.64	2.99	15.10 14.38[a)]	3.08 3.05[a)]

a) Calculated with the same structure as that for ΔN = 0.0, i.e., EF = 0.0 V/nm.

Table II. Structure of the BeO/Pt/TM/Pt(111) (TM=Fe, Co) system for the change in electron number ΔN=−0.1, 0.0, and 0.1. The x and y coordinates (in Å) are chosen according to the lattice constant of the Pt(111) underlayer with the in-plane primitive vectors $\boldsymbol{a}_1 = (a, 0, 0)$ and $\boldsymbol{a}_2 = (-a/2, \sqrt{3}a/2, 0)$ where a=2.77 Å. The z coordinates (in Å) are optimized under the electric field of $-0.272\,\Delta N \times 10^3$ V/nm with the definition that a positive (negative) electric field decreases (increases) the number of electrons in the system.

				z		
System	Atom	x	y	$\Delta N = -0.1$	$\Delta N = 0.0$	$\Delta N = 0.1$
BeO/Pt/Fe/Pt(111)	Be	1.39	0.80	6.84	6.81	6.84
	O	0.00	1.60	6.28	6.31	6.39
	Be	0.00	1.60	4.70	4.69	4.71
	O	1.39	0.80	4.17	4.22	4.30
	Pt	1.39	0.80	2.04	2.04	2.05
	Fe	0.00	0.00	0.00	0.00	0.00
	Pt(I)	1.39	0.80	−2.04	−2.04	−2.04
	Pt(II)	0.00	0.00	−4.38	−4.38	−4.39
BeO/Pt/Co/Pt(111)	Be	1.39	0.80	6.80	6.76	6.79
	O	0.00	1.60	6.24	6.26	6.35
	Be	0.00	1.60	4.66	4.64	4.66
	O	1.39	0.80	4.13	4.17	4.25
	Pt	1.39	0.80	2.00	2.00	2.01
	Co	0.00	0.00	0.00	0.00	0.00
	Pt(I)	1.39	0.80	−2.01	−2.01	−2.02
	Pt(II)	0.00	0.00	−4.34	−4.34	−4.34

Table III. Numbers of majority- and minority-spin electrons, N^+ and N^-, and the difference, $N^+ - N^-$, of the O atom on top of the segregated Pt atom (O), the segregated Pt atom (Pt), the TM atom (Fe, Co), and the first and second Pt underlayer atoms (Pt(I) and Pt(II)) in the BeO/Pt/TM/Pt(111) systems for the change in electron number ΔN=−0.1, 0.0, and 0.1. Note that $N^+ - N^-$ represents the atomic spin magnetic moment in unit of μ_B. The electric field, EF (in V/nm), is given by $-0.272\,\Delta N \times 10^3$ V/nm, with the definition that a positive (negative) electric field decreases (increases) the number of electrons in the system.

		$\Delta N = -0.1$ (EF = 27.2)			$\Delta N = 0.0$ (EF = 0.0)			$\Delta N = 0.1$ (EF = −27.2)		
System	Atom	N^+	N^-	$N^+ - N^-$	N^+	N^-	$N^+ - N^-$	N^+	N^-	$N^+ - N^-$
BeO/Pt/Fe/Pt(111)	O	4.32	4.35	−0.03	4.33	4.35	−0.02	4.34	4.33	0.01
	Pt	38.94	38.78	0.16	38.98	38.78	0.20	39.03	38.77	0.26
	Fe	14.41	11.69	2.72	14.42	11.66	2.76	14.44	11.63	2.81
	Pt(I)	39.10	38.83	0.27	39.09	38.84	0.25	39.09	38.84	0.25
	Pt(II)	39.03	39.00	0.03	39.03	39.01	0.02	39.02	39.01	0.01
BeO/Pt/Co/Pt(111)	O	4.36	4.32	0.04	4.36	4.32	0.04	4.36	4.31	0.05
	Pt	39.03	38.70	0.33	39.09	38.68	0.41	39.12	38.68	0.44
	Co	14.51	12.58	1.93	14.53	12.55	1.98	14.54	12.53	2.01
	Pt(I)	39.15	38.79	0.36	39.16	38.77	0.39	39.17	38.77	0.40
	Pt(II)	39.08	38.94	0.14	39.09	38.93	0.16	39.10	38.93	0.17

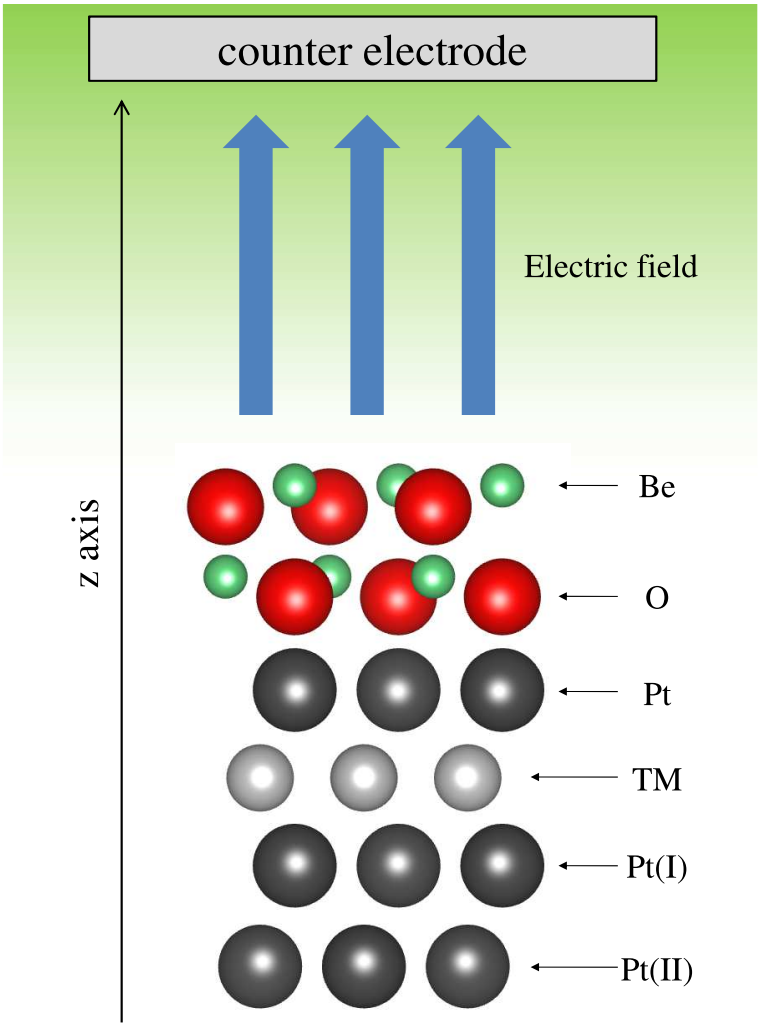

Fig. 1. (Color online) Schematic diagram of the BeO/Pt/TM/Pt(111) system where TM=Fe, Co. The system consists of the BeO insulating layer, the segregated Pt monolayer, the TM monolayer, and the Pt(111) underlayer where the first and second Pt underlayer atoms are denoted by Pt(I) and Pt(II), respectively. The electric field is applied by introducing the counter electrode far above the system. The direction of the electric field is defined in such a way that a positive (negative) electric field decreases (increases) the number of electrons in the system, pointing upward (downward) along the positive (negative) z axis direction.

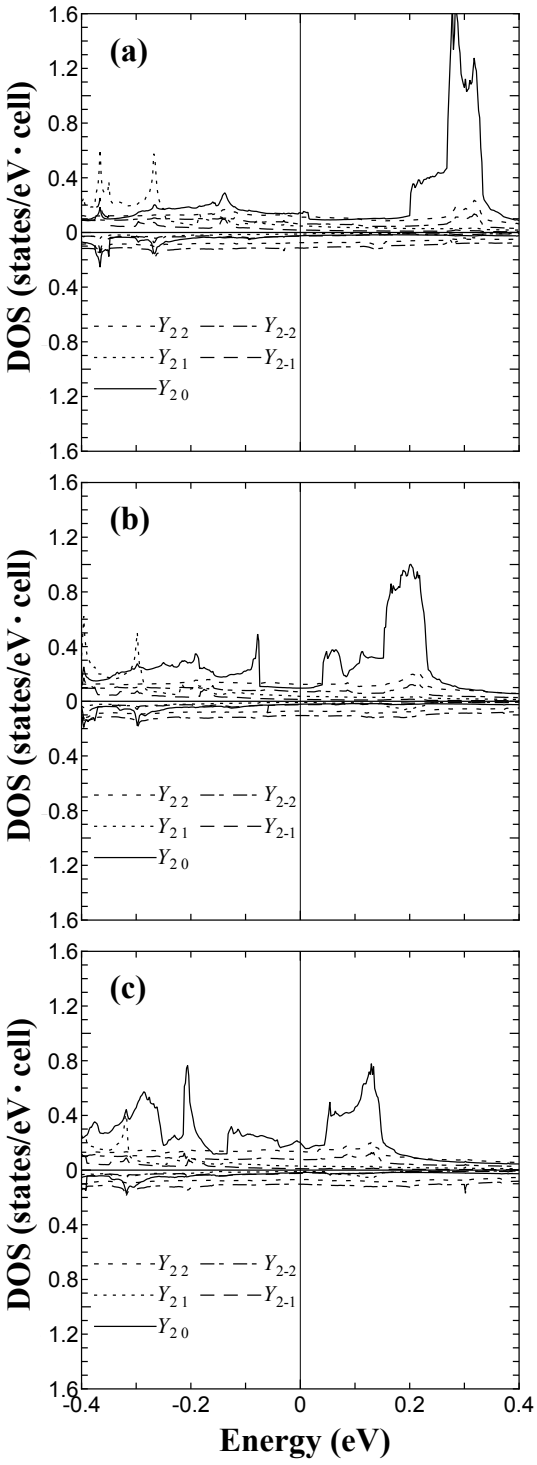

Fig. 2. Partial density of states of the 5*d* orbitals of the segregated Pt atom in the BeO/Pt/Fe/Pt(111) system for (a)ΔN=−0.1 (EF=27.2 V/nm), (b)ΔN=0.0 (EF=0.0 V/nm), and (c)ΔN=0.1 (EF=−27.2 V/nm), where ΔN represents the change in the number of electrons in the system. The upper and lower parts of each panel are those for majority- and minority-spin orbitals, respectively. The PDOS of the Pt 5*d* orbitals are labeled with Y_{lm} of l = 2 and m = ±2, ±1, and 0. Note that Y_{20} represents the Pt $5d_{3z^2-r^2}$ orbital. The zero of energy is taken as the Fermi level.

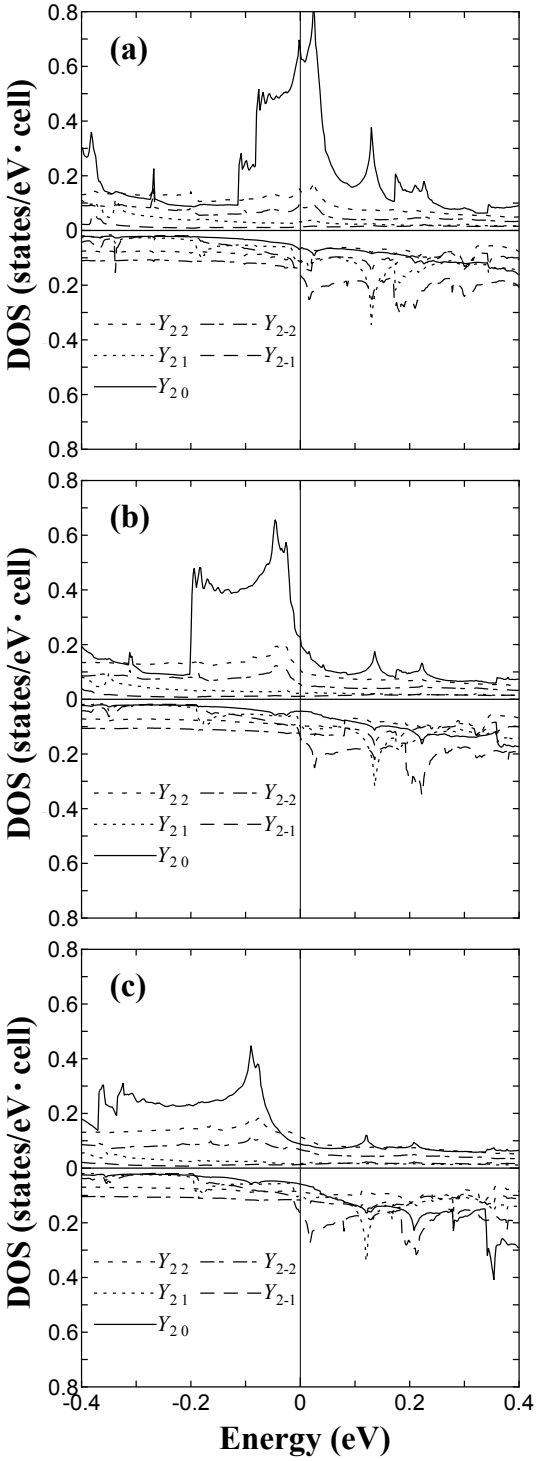

Fig. 3. Partial density of states of the 5*d* orbitals of the segregated Pt atom in the BeO/Pt/Co/Pt(111) system for (a)ΔN=−0.1 (EF=27.2 V/nm), (b)ΔN=0.0 (EF=0.0 V/nm), and (c)ΔN=0.1 (EF=−27.2 V/nm), where ΔN represents the change in the number of electrons in the system. The upper and lower parts of each panel are those for majority- and minority-spin orbitals, respectively. The PDOS of the Pt 5*d* orbitals are labeled with Y_{lm} of l = 2 and m = ±2, ±1, and 0. Note that Y_{20} represents the Pt $5d_{3z^2-r^2}$ orbital. The zero of energy is taken as the Fermi level.

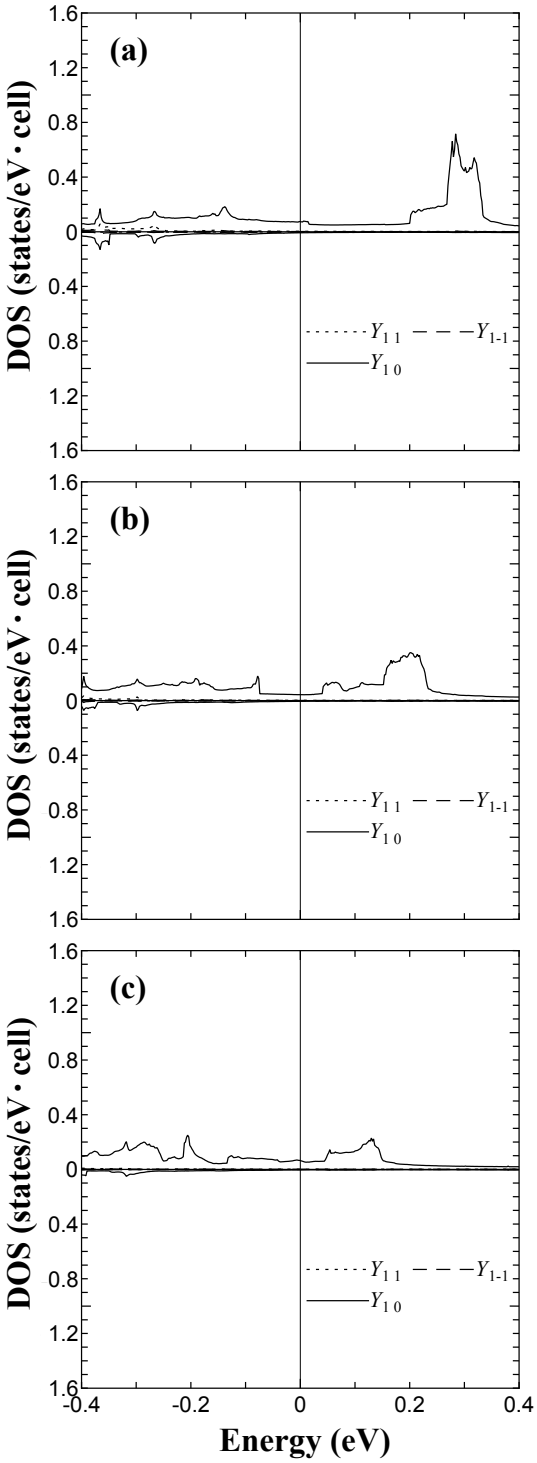

Fig. 4. Partial density of states of the $2p$ orbitals of the O atom on top of the segregated Pt atom in the BeO/Pt/Fe/Pt(111) system for (a)ΔN=−0.1 (EF=27.2 V/nm), (b)ΔN=0.0 (EF=0.0 V/nm), and (c)ΔN=0.1 (EF=−27.2 V/nm), where ΔN represents the change in the number of electrons in the system. The upper and lower parts of each panel are those for majority- and minority-spin orbitals, respectively. The PDOS of the O $2p$ orbitals are labeled with Y_{lm} of l = 1 and m = ±1, and 0. Note that Y_{10} represents the O $2p_z$ orbital. The zero of energy is taken as the Fermi level.

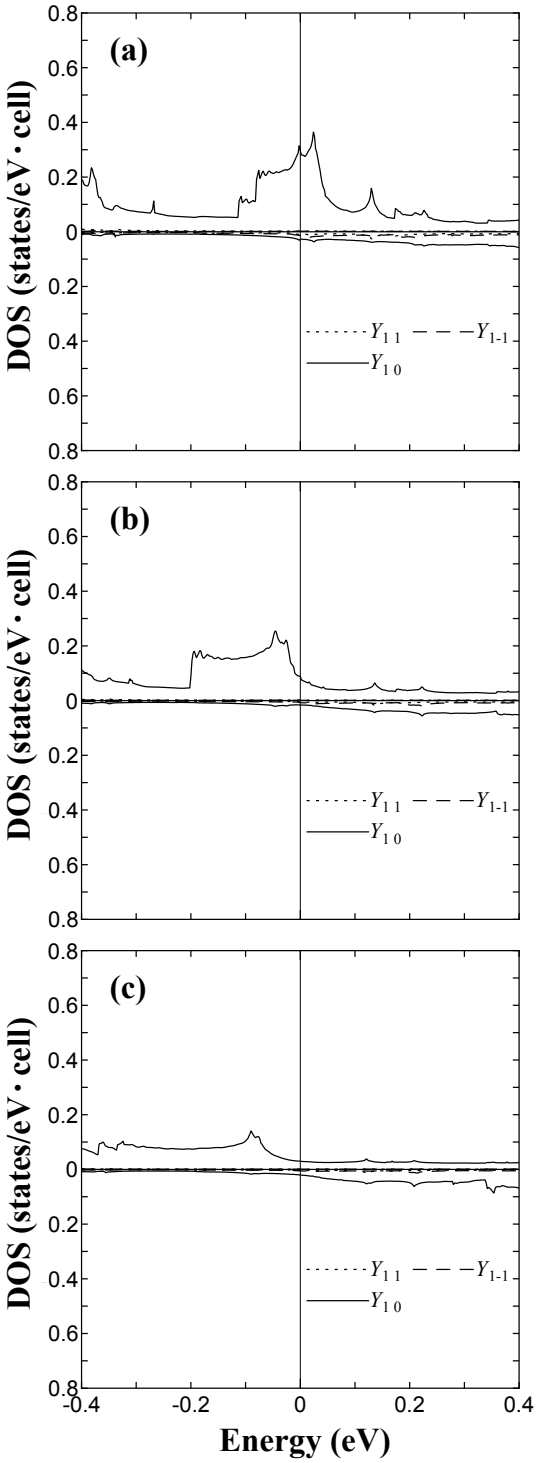

Fig. 5. Partial density of states of the $2p$ orbitals of the O atom on top of the segregated Pt atom in the BeO/Pt/Co/Pt(111) system for (a)ΔN=−0.1 (EF=27.2 V/nm), (b)ΔN=0.0 (EF=0.0 V/nm), and (c)ΔN=0.1 (EF=−27.2 V/nm), where ΔN represents the change in the number of electrons in the system. The upper and lower parts of each panel are those for majority- and minority-spin orbitals, respectively. The PDOS of the O $2p$ orbitals are labeled with Y_{lm} of l = 1 and m = ±1, and 0. Note that Y_{10} represents the O $2p_z$ orbital. The zero of energy is taken as the Fermi level.

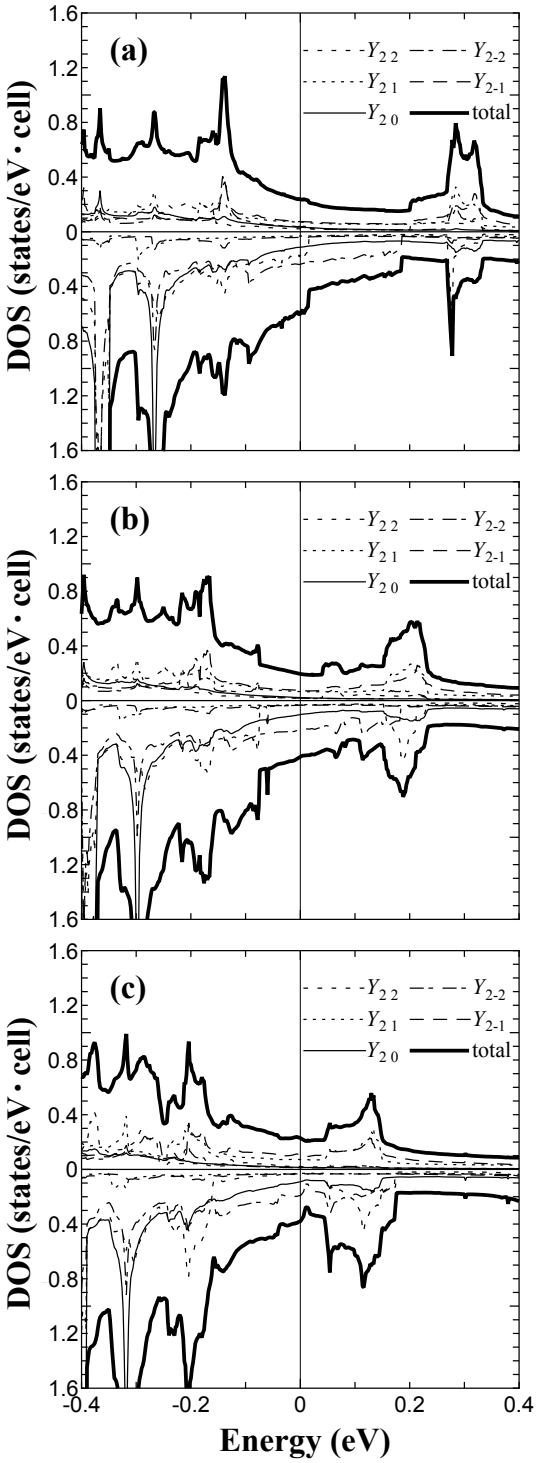

Fig. 6. Partial density of states of the 3*d* orbitals of the Fe atom in the BeO/Pt/Fe/Pt(111) system for (a)ΔN=−0.1 (EF=27.2 V/nm), (b)ΔN=0.0 (EF=0.0 V/nm), and (c)ΔN=0.1 (EF=−27.2 V/nm), where ΔN represents the change in the number of electrons in the system. The upper and lower parts of each panel are those for majority- and minority-spin orbitals, respectively. The PDOS of the Fe 3*d* orbitals are labeled with Y_{lm} of l = 2 and m = ±2, ±1, and 0. The total partial density of states of the 3*d* orbitals of the Fe atom is shown with the thick solid line. The zero of energy is taken as the Fermi level.

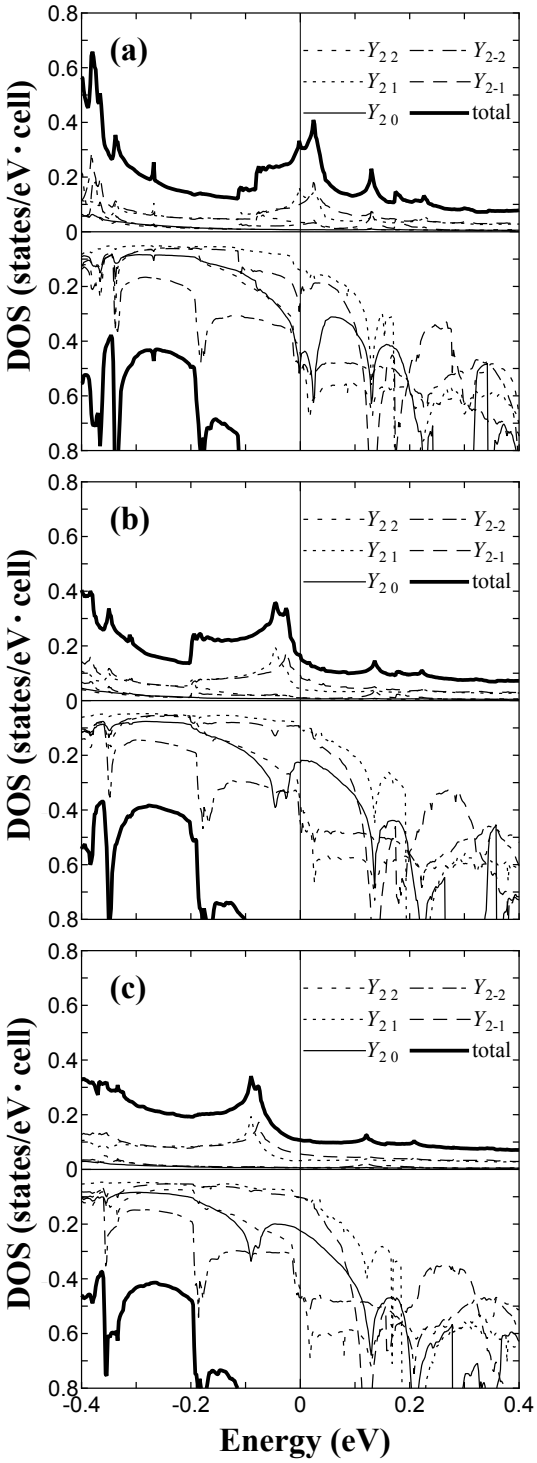

Fig. 7. Partial density of states of the 3*d* orbitals of the Co atom in the BeO/Pt/Co/Pt(111) system for (a)ΔN=−0.1 (EF=27.2 V/nm), (b)ΔN=0.0 (EF=0.0 V/nm), and (c)ΔN=0.1 (EF=−27.2 V/nm), where ΔN represents the change in the number of electrons in the system. The upper and lower parts of each panel are those for majority- and minority-spin orbitals, respectively. The PDOS of the Co 3*d* orbitals are labeled with Y_{lm} of l = 2 and m = ±2, ±1, and 0. The total partial density of states of the 3*d* orbitals of the Co atom is shown with the thick solid line. The zero of energy is taken as the Fermi level.

References

1) *Ultrathin Magnetic Structures*, ed. J. A. C. Bland and B. Heinrich (Springer-Verlag Berlin Heidelberg, 1994 and 2005) Vol. I-II and III-IV.

2) H. Ohno, D. Chiba, F. Matsukura, T. Omiya, E. Abe, T. Dietl, Y. Ohno, and K. Ohtani, Nature **408**, 944 (2000).

3) D. Chiba, M. Yamanouchi, F. Matsukura, and H. Ohno, Science **301**, 943 (2003).

4) D. Chiba, M. Sawicki, Y. Nishitani, Y. Nakatani, F. Matsukura, and H. Ohno, Nature **455**, 515 (2008).

5) M. Weisheit, S. Fähler, A. Marty, Y. Souche, C. Poinsignon, and D. Givord, Science **315**, 349 (2007).

6) T. Maruyama, Y. Shiota, T. Nozaki, K. Ohta, N. Toda, M. Mizuguchi, A. A. Tulapurkar, T. Shinjo, M. Shiraishi, S. Mizukami, Y. Ando, and Y. Suzuki, Nature Nanotech. **4**, 158 (2009).

7) K. Ohta, T. Maruyama, T. Nozaki, M. Shiraishi, T. Shinjo, Y. Suzuki, S.-S. Ha, C.-Y. You, and W. Van Roy, Appl. Phys. Lett. **94**, 032501 (2009).

8) Y. Shiota, T. Maruyama, T. Nozaki, T. Shinjo, M. Shiraishi, and Y. Suzuki, Appl. Phys. Express **2**, 063001 (2009).

9) T. Nozaki, Y. Shiota, M. Shiraishi, T. Shinjo, and Y. Suzuki, Appl. Phys. Lett. **96**, 022506 (2010).

10) S.-S. Ha, N.-H. Kim, S. Lee, C.-Y. You, Y. Shiota, T. Maruyama, T. Nozaki, and Y. Suzuki, Appl. Phys. Lett. **96**, 142512 (2010).

11) M. Endo, S. Kanai, S. Ikeda, F. Matsukura, and H. Ohno, Appl. Phys. Lett. **96**, 212503 (2010).

12) M. Zhernenkov, M. R. Fitzsimmons, J. Chlistunoff, and J. Majewski, Phys. Rev. B **82**, 024420 (2010).

13) D. Chiba, S. Fukami, K. Shimamura, N. Ishiwata, K. Kobayashi, and T. Ono, Nature Mater. **10**, 853 (2011).

14) T. Seki, M. Kohda, J. Nitta, and K. Takanashi, Appl. Phys. Lett. **98**, 212505 (2011).

15) F. Bonell, S. Murakami, Y. Shiota, T. Nozaki, T. Shinjo, and Y. Suzuki, Appl. Phys. Lett. **98**, 232510 (2011).

16) Y. Shiota, S. Murakami, F. Bonell, T. Nozaki, T. Shinjo, and Y. Suzuki, Appl. Phys. Express **4**, 043005 (2011).

17) Y. Shiota, T. Nozaki, F. Bonell, S. Murakami, T. Shinjo, and Y. Suzuki, Nature Mater. **11**, 39 (2012).

18) W.-G. Wang, M. Li, S. Hageman, and C. L. Chien, Nature Mater. **11**, 64 (2012).

19) T. Nozaki, Y. Shiota, S. Miwa, S. Murakami, F. Bonell, S. Ishibashi, H. Kubota, K. Yakushiji, T. Saruya, A. Fukushima, S. Yuasa, T. Shinjo, and Y. Suzuki, Nature Physics **8**, 491 (2012).

20) K. Shimamura, D. Chiba, S. Ono, S. Fukami, N. Ishiwata, M. Kawaguchi, K. Kobayashi, and T. Ono, Appl. Phys. Lett. **100**, 122402 (2012).

21) S. Kanai, M. Yamanouchi, S. Ikeda, Y. Nakatani, F. Matsukura, and H. Ohno, Appl. Phys. Lett. **101**, 122403 (2012).

22) M. Kawaguchi, K. Shimamura, S. Ono, S. Fukami, F. Matsukura, H. Ohno, D. Chiba, and T. Ono, Appl. Phys. Express **5**, 063007 (2012).

23) D. Chiba, M. Kawaguchi, S. Fukami, N. Ishiwata, K. Shimamura, K. Kobayashi, and T. Ono, Nature Commun. **3**, 888 (2012).

24) F. Bonell, Y. T. Takahashi, D. D. Lam, S. Yoshida, Y. Shiota, S. Miwa, T. Nakamura, and Y. Suzuki, Appl. Phys. Lett. **102**, 152401 (2013).

25) Y. Shiota, F. Bonell, S. Miwa, N. Mizuochi, T. Shinjo, and Y. Suzuki, Appl. Phys. Lett. **103**, 082410 (2013).

26) K. Yamada, H. Kakizakai, K. Shimamura, M. Kawaguchi, S. Fukami, N. Ishiwata, D. Chiba, and T. Ono, Appl. Phys. Express **6**, 073004 (2013).

27) T. Nozaki, K. Yakushiji, S. Tamaru, M. Sekine, R. Matsumoto, M. Konoto, H. Kubota, A. Fukushima, and S. Yuasa, Appl. Phys. Express **6**, 073005 (2013).

28) T. Koyama, A. Obinata, Y. Hibino, and D. Chiba, Appl. Phys. Express **6**, 123001 (2013).

29) C. G. Duan, J. P. Velev, R. F. Sabirianov, Z. Zhu, J. Chu, S. S. Jaswal, and E. Y. Tsymbal, Phys. Rev. Lett. **101**, 137201 (2008).

30) K. Nakamura, R. Shimabukuro, Y. Fujiwara, T. Akiyama, T. Ito, and A. J. Freeman, Phys. Rev. Lett. **102**, 187201 (2009).

31) K. Nakamura, R. Shimabukuro, T. Akiyama, T. Ito, and A. J. Freeman, Phys. Rev. B **80**, 172402 (2009).

32) M. Tsujikawa and T. Oda, Phys. Rev. Lett. **102**, 247203 (2009).

33) H. Zhang, M. Richter, K. Koepernik, I. Opahle, F. Tasnádi, and H. Eschrig, New J. Phys. **11**, 043007 (2009).

34) K. Nakamura, T. Akiyama, T. Ito, M. Weinert, and A. J. Freeman, Phys. Rev. B **81**, 220409 (2010).

35) M. K. Niranjan, C. G. Duan, S. S. Jaswal, and E. Y. Tsymbal, Appl. Phys. Lett. **96**, 222504 (2010).

36) R. Shimabukuro, K. Nakamura, T. Akiyama, and T. Ito, Physica E **42**, 1014 (2010).

37) M. Tsujikawa, S. Haraguchi, T. Oda, Y. Miura, and M. Shirai, J. Appl. Phys. **109**, 07C107 (2011).

38) S. Haraguchi, M. Tsujikawa, J. Gotou, and T. Oda, J. Phys. D, Appl. Phys. **44**, 064005 (2011).

39) M. Tsujikawa, S. Haraguchi, and T. Oda, J. Appl. Phys. **111**, 083910 (2012).

40) S. Yasuda and S. Suzuki, J. Phys. Soc. Jpn. **81**, 085002 (2012).

41) S. Suzuki, S. Yasuda, K. Edakawa, and S. Seki, J. Phys. Soc. Jpn. **82**, 124715 (2013).

42) C. Kittel: *Introduction to Solid State Physics* (Wiley, New York, 2005) 8th ed., p. 325.

43) C. A. Menning, H. H. Hwu, and J. G. Chen, J. Phys. Chem. B **110**, 15471 (2006).

44) C. A. Menning and J. G. Chen, J. Chem. Phys. **128**, 164703 (2008).

45) S. Suzuki and K. Nakao, J. Phys. Soc. Jpn. **66**, 3881 (1997).

46) S. Suzuki and K. Nakao, J. Phys. Soc. Jpn. **68**, 1982 (1999).

47) S. Suzuki and K. Nakao, J. Phys. Soc. Jpn. **69**, 532 (2000).

48) D. M. Ceperley and B. J. Alder, Phys. Rev. Lett. **45**, 566 (1980).

49) J. P. Perdew and Y. Wang, Phys. Rev. B **45**, 13244 (1992).

50) D. E. Parry, Surf. Sci. **49**, 433 (1975).

51) F. E. Harris, Int. J. Quantum Chem. **68**, 385 (1998).

52) E. Kaxiras, Y. Bar-Yam, and D. Joannopoulos, Phys. Rev. B **33**, 4406 (1986).

53) K. Shiraishi, J. Phys. Soc. Jpn. **59**, 3455 (1990).

54) L.-K. Hua and Y. Wang, *Applications of Number Theory to Numerical Analysis* (Springer-Verlag, Berlin, 1981).

55) M. Tsujikawa, A. Hosokawa, and T. Oda, J. Phys., Condens. Matter **19**, 365208 (2007).

56) G. Moulas, A. Lehnert, S. Rusponi, J. Zabloudil, C. Etz, S. Ouazi, M. Etzkorn, P. Bencok, P. Gambardella, P. Weinberger, and H. Brune, Phys. Rev. B **78**, 214424 (2008).

57) A. Lehnert, S. Dennler, P. Błoński, S. Rusponi, M. Etzkorn, G. Moulas, P. Bencok, P. Gambardella, H. Brune, and J. Hafner, Phys. Rev. B **82**, 094409 (2010).

58) D. Repetto, T. Y. Lee, S. Rusponi, J. Honolka, K. Kuhnke, V. Sessi, U. Starke, H. Brune, P. Gambardella, C. Carbone, A. Enders, and K. Kern, Phys. Rev. B **74**, 054408 (2006).

59) P. Gambardella, S. Rusponi, M. Veronese, S. S. Dhesi, C. Grazioli, A. Dallmeyer, I. Cabria, R. Zeller, P. H. Dederichs, K. Kern, C. Carbone, and H. Brune, Science **300**, 1130 (2003).

60) A. Szabo and N. S. Ostlund: *Modern Quantum Chemistry: Introduction to Advanced Electronic Structure Theory* (Dover Publicatsions, New York, 1996) 1st ed., p. 151.